ChemComm

FEATURE ARTICLE

View Article Online
View Journal | View Issue

Cite this: *Chem. Commun.*, 2025, **61**, 10716

Powering the extreme: rising world of batteries that could operate at ultra-low temperatures

Sung-Kwang Jung,†[a] Jyotirekha Dutta,†[ab] Surendra K. Martha,[b] Martin Byung-Guk Jun[c] and Vilas G. Pol*[a]

Rechargeable lithium-ion batteries and sodium-ion batteries significantly underperform at ultra-low temperatures, limiting their applicability in critical fields such as aerospace, polar exploration, and cold-climate electric vehicles. This review summarizes recent progress in overcoming these challenges by advancing key battery components: electrolyte, electrode, and separator. Improvements in electrolyte formulations focus on solvation dynamics to enhance ionic conductivity and operational stability under sub-zero conditions. Electrode designs are employed by developing multicomponent materials, structure and interface engineering, and morphology control to effectively alleviate kinetic limitations and suppress detrimental side reactions. Separator modifications introduce functional surface coatings to broaden the operational temperature range while improving safety characteristics. Finally, this review provides a comprehensive overview and future research directions to enable the practical deployment of robust battery technologies for extreme-temperature applications.

Received 24th April 2025,
Accepted 29th May 2025

DOI: 10.1039/d5cc02279g

rsc.li/chemcomm

1. Introduction

Rechargeable batteries are critical for modern energy storage applications, including electric vehicles (EVs), portable electronics, and grid-scale energy storage. Among them, lithium-ion batteries (LIBs) are one of the most widely studied and implemented technologies due to their high energy density, long cycle life, and efficient charge/discharge characteristics. However, such battery systems face significant performance degradation in low-temperature environments, which limits their applications in extreme climate conditions, such as aerospace, polar regions, and winter-intensive climates. However, to mitigate the cost and resource constraints of lithium-based systems, sodium-ion batteries (SIBs) have emerged as a promising alternative, especially for large-scale energy storage. Nonetheless, SIBs

[a] *Davidson School of Chemical Engineering, Purdue University, West Lafayette, IN, 47907, USA. E-mail: vpol@purdue.edu*
[b] *Department of Chemistry, Indian Institute of Technology Hyderabad, Kandi, Sangareddy, 502284, Telangana, India*
[c] *School of Mechanical Engineering, Purdue University, West Lafayette, IN, 47907, USA*
† Both authors contributed equally to this work.

Sung-Kwang Jung

Sung-Kwang Jung received his BSc degree in Chemical Engineering in 2020 and his MSc degree in Nano Science and Technology in 2022, both from Sungkyunkwan University, South Korea. He is currently pursuing his PhD in Chemical Engineering at Purdue University, USA, under the supervision of Dr Vilas G. Pol. His research focuses on advanced electrolyte design and electrode engineering strategies to enable ultra-low-temperature operation of lithium-ion batteries.

Jyotirekha Dutta

Jyotirekha Dutta received her BSc degree in Chemistry from Dibrugarh University, Assam, India, in 2018, and her MSc degree in Chemistry from Gauhati University, Assam, India, in 2020. Currently, she is a PhD student at Indian Institute of Technology, Hyderabad (India) under the supervision of Dr Surendra Kumar Martha. She is also currently working as a visiting scholar at Purdue University, USA, under the supervision of Dr Vilas G. Pol. Her main research interests are focused on low to no co-based cathodes for Li-ion batteries and wide temperature electrolyte study for sodium-ion batteries.

also experience substantial performance degradation in extreme conditions.

At sub-zero temperatures, both LIBs and SIBs exhibit limitations in electrolyte systems and electrode materials, especially in terms of battery kinetics, stability, and safety, which necessitate compensation for degraded performance and expand the operational temperature window.[1] Electrolyte freezing, sluggish ion diffusion, increased charge-transfer resistance (R_{ct}), and unstable solid electrolyte interphase (SEI) formation contribute to capacity fading, voltage hysteresis, and safety concerns, including lithium or sodium metal plating. The commonly used carbonate-based electrolytes suffer from poor ionic conductivity at low temperatures, while electrode materials exhibit deteriorated charge storage and transport properties, further limiting overall battery efficiency. Addressing these challenges requires sophisticated anode, cathode, electrolyte selection, and structure design to improve charge kinetics and interfacial stability.

Recent research has focused on several strategies to enhance low-temperature performance in both LIBs and SIBs.[2–6] Electrolyte engineering has led to advancements such as the design of solvation structure and chemistry, advanced electrolyte systems, interphase optimization, and the introduction of polymer or quasi-solid-state species, which provide improved ionic conductivity and interfacial stability. Electrode material has explored strategies such as multicomponent materials, novel structural and interfacial engineering, and morphological modifications to optimize structural and electronic properties to mitigate freezing issues and improve thermal stability. Finally, separator modifications and system-level thermal management strategies further contribute to enhancing battery performance in extreme environments.

This review presents a comprehensive discussion of LIBs and SIBs for low-temperature applications by comparing recent advancements in electrolyte formulations, electrode material modifications, and innovative electrochemical strategies with the research work of our team. We highlighted key innovations in electrolyte formulation, including approaches that enhance ion transport and interfacial stability, which are critical for maintaining battery function in cold environments. Additionally, advancements in electrode design including the use of composite materials and structural optimization are discussed for their role in supporting stable and efficient electrochemical reactions at low temperatures. The scope further extends to

Surendra K. Martha

Surendra K. Martha is a professor and head of the Department of Chemistry, Indian Institute of Technology, Hyderabad (IIT H) (India). He graduated in 2006 from the Indian Institute of Science, Bangalore, India, under the supervision of Dr Ashok K. Shukla. Previously, Dr Martha worked as a Postdoctoral Research Associate at the Oak Ridge National Laboratory, Tennessee, USA, and Bar-Ilan University, Israel. His recent research interests are in materials electrochemistry with particular emphasis on Li-ion, Na-ion, Li–S, dual carbon, lead–acid, supercapacitors, Li/Na ion non-aqueous capacitors, MXenes, and recycling Li-ion batteries. He has over 146 publications (h-index 38) in peer-reviewed Materials Science and Electrochemistry Journals and over 16 patents, 16 book chapters, and has contributed to over 110 academic conferences.

Martin Byung-Guk Jun

Martin Byung-Guk Jun is a Professor of the School of Mechanical Engineering at Purdue University, West Lafayette, IN, USA. He is also the Director of the Center of Operation and Research for Industry Advancement (CORIA) and a Co-Director of the Smart Manufacturing Innovation Center (SMIC) at Purdue. He has authored over 190 peer-reviewed journal publications. He is an ASME fellow and Area Editor of Journal of Manufacturing Processes. He is also the recipient of the 2011 SME Outstanding Young Manufacturing Engineer Award, 2012 Canadian Society of Mechanical Engineers I. W. Smith Award for Outstanding Achievements, 2015 Korean Society of Manufacturing Technology Engineers Damwoo Award, and 2023 Italian Machine Tool Technology Award. He has also been recognized as 20 most influential academics and 25 leaders transforming manufacturing in the Smart Manufacturing magazine.

Vilas G. Pol

Vilas G. Pol is a Professor of Chemical Engineering at Purdue University, IN, USA. He has authored/co-authored over 285 research publications (h-index 62) and is an inventor on 27 issued US patents with 10^{+} additional applications. He has delivered hundreds of invited, keynote, and plenary talks, including a TEDx presentation. Purdue University has honored him with Outstanding Engineering Teacher, Most Impactful Inventor, Seed for Success, Bravo, and Purdue Faculty Scholar awards. He has received more than 40 prestigious awards from professional societies including AIChE, ACS, MRS, ACerS, TMS, and Carbon. His accolades include a 2015 R&D 100 award, Intel Prize, two Guinness World Records™, Fellow of the Royal Society of Chemistry (FRSC), and a Fulbright Specialist.

system-level strategies, such as separator modification, to enhance ionic transport and maintain mechanical robustness under thermal stress. By benchmarking these developments against our previous research, this review not only identifies persistent limitations but also articulates a practical roadmap for the rational design of next-generation rechargeable batteries engineered for reliable performance in ultra-low temperature environments.

2. Electrolyte engineering

Conventional electrolytes, typically based on carbonate solvents such as ethylene carbonate (EC), exhibit several limitations at sub-zero temperatures.[7,8] These solvents have high freezing points (36 °C for EC) that facilitate electrolyte freezing and poor ionic conductivity, severely impairing ion transport and increasing internal resistance. Additionally, at low temperatures, sluggish ion desolvation kinetics and inefficient SEI formation result in high R_{ct}, poor rate capability, and lithium plating, which compromises battery safety and cycle life. Therefore, delicate electrolyte design is essential to minimize such adverse effects while maintaining high ionic conductivity and innocuous interfacial reactions. Recent studies have focused on strategies including solvent design, solvation structure optimization, electrode–electrolyte interphase modulation, and novel electrolyte compositions.[9,10]

2.1. Solvent engineering and solvation structure design

Solvent engineering aims to optimize molecular interactions, interfacial behavior, and transport kinetics to ensure reliable electrolyte functionalities. Under low temperatures, retarded kinetics and aggregation of ions and solvent molecules induce several side effects, such as salt precipitation, decreased ionic conductivity, and limited liquid-state of electrolytes. Therefore, effective electrolyte design relies on precise control between fundamental solvent properties, including freezing point, viscosity, dielectric constant, and solvation strength. A well-established electrolyte should demonstrate sufficient fluidity at low temperatures while retaining efficient Li^+/Na^+ transport and stable electrode interfaces. More specifically, the choice of solvents must account for their ability to facilitate Li^+ dissociation while preventing excessive solvation that could hinder ion mobility. The formation of solvation structures is affected by a balance between ion–ion, ion–solvent (ion–dipole), and solvent–solvent (dipole–dipole) interactions. Solvation structure engineering thus focuses on optimizing the bulk properties of electrolytes through strategies such as ion-coordination control. Furthermore, beneficial solvent–electrode interactions play a crucial role in the formation of a stable SEI on anodes and a protective cathode electrolyte interphase (CEI) that suppresses side reactions. By tuning molecular structure and composition, studies aimed to enhance the physical and electrochemical stability of the electrolyte without compromising its conductivity or compatibility with electrode materials.

Notably, cyclopentyl methyl ether (CPME)[11] has been identified as one of the promising electrolyte solvents, primarily due to its ultra-low freezing point (−140 °C) and unique solvation characteristics. The weak solvating ability of CPME promotes the coordination of Li^+ with anions, leading to the formation of high-concentration coordination clusters. This distinctive solvation structure facilitates the development of a stable, lithium fluoride (LiF)-rich SEI, which enhances Li^+ transport and charge transfer kinetics at low temperatures. As a result, recent studies have demonstrated that CPME-based electrolytes enable LIBs to retain initial capacity and facilitate stable cycling. Ramasamy *et al.* validated that CPME enables stable lithium intercalation without freezing at −40 °C, leveraging its low freezing point and weak solvating nature to optimize Li^+ transport.[11] CPME forms a contact ion pair (CIP) and aggregate (AGG) dominated solvation structure, which improves Li^+ mobility and desolvation kinetics. Raman spectroscopy revealed that in CIP structures, Li^+ coordinates directly with FSI^- anions, reducing solvent-shell thickness and lowering desolvation energy (69.6 kJ mol^{-1}) (Fig. 1a and b). Moreover, AGG structures incorporate multiple anions per Li^+, promoting intra-aggregate ion exchange, further accelerating charge transfer kinetics and minimizing interfacial polarization. Electrochemical impedance spectroscopy (EIS) further confirmed that CIP/AGG solvation significantly reduced R_{ct}, enabling stable Li^+ intercalation without plating (Fig. 1c and d). Furthermore, a unique solvation structure of lithium bis(fluorosulfonyl)imide (LiFSI) in CPME facilitates the formation of a thin, LiF-rich SEI, enhancing ion transport and reducing R_{ct}. As a result, Li‖graphite half-cells with 1 M LiFSI in CPME retained 100% capacity at −20 °C and delivered 274 mA h g^{-1} at −40 °C, far excelling conventional electrolytes. In another study, Jamison *et al.* introduced a customized extreme low-temperature system (ELTS) to test Li‖$Li_4Ti_5O_{12}$ (LTO) cells with 1 M LiFSI in CPME electrolyte across various temperatures.[12] Combined with the CPME-based electrolyte, LTO anode maintained exceptional operational stability due to its zero-strain Li^+ insertion/extraction, which suppressed volume expansion and phase transitions to ensure efficient charge transfer at ultra-low temperatures. The cells delivered discharge capacities of 159 mA h g^{-1} at room temperature, 119 mA h g^{-1} at −20 °C, 101 mA h g^{-1} at −40 °C, and 33 mA h g^{-1} at −60 °C, with 7.12 mA h g^{-1} at −100 °C, marking the first-ever demonstration of LIB operation at such extreme temperature conditions (Fig. 1e–h). By employing ELTS, in the following study, Kim *et al.* suggested a niobium tungsten oxide (NbWO) electrode coupled with tailored CPME electrolytes to enable cycling at −100 °C and beyond.[13] The pseudocapacitive NbWO material exhibited a homogeneous Nb and W distribution, preventing Li ordering and facilitating fast Li^+ diffusion within the electrode lattice. The NbWO anode demonstrated exceptional low-temperature performance, retaining 75 mA g^{-1} at −100 °C and remaining operable at −120 °C. The multielectron redox reactions (Nb^{5+}/Nb^{4+} and W^{6+}/W^{5+}) further improved capacity retention and stability. CPME electrolytes maintained low viscosity and facile Li^+ desolvation, preventing freezing and ensuring stable ion transport. Another work applied solvation structure design to minimize the polysulfide shuttle effect within Li–S batteries. Das *et al.* utilized the role of lithium nitrate ($LiNO_3$) as a high-donor number nitrate salt to interact with lithium polysulfides and alter the solvation

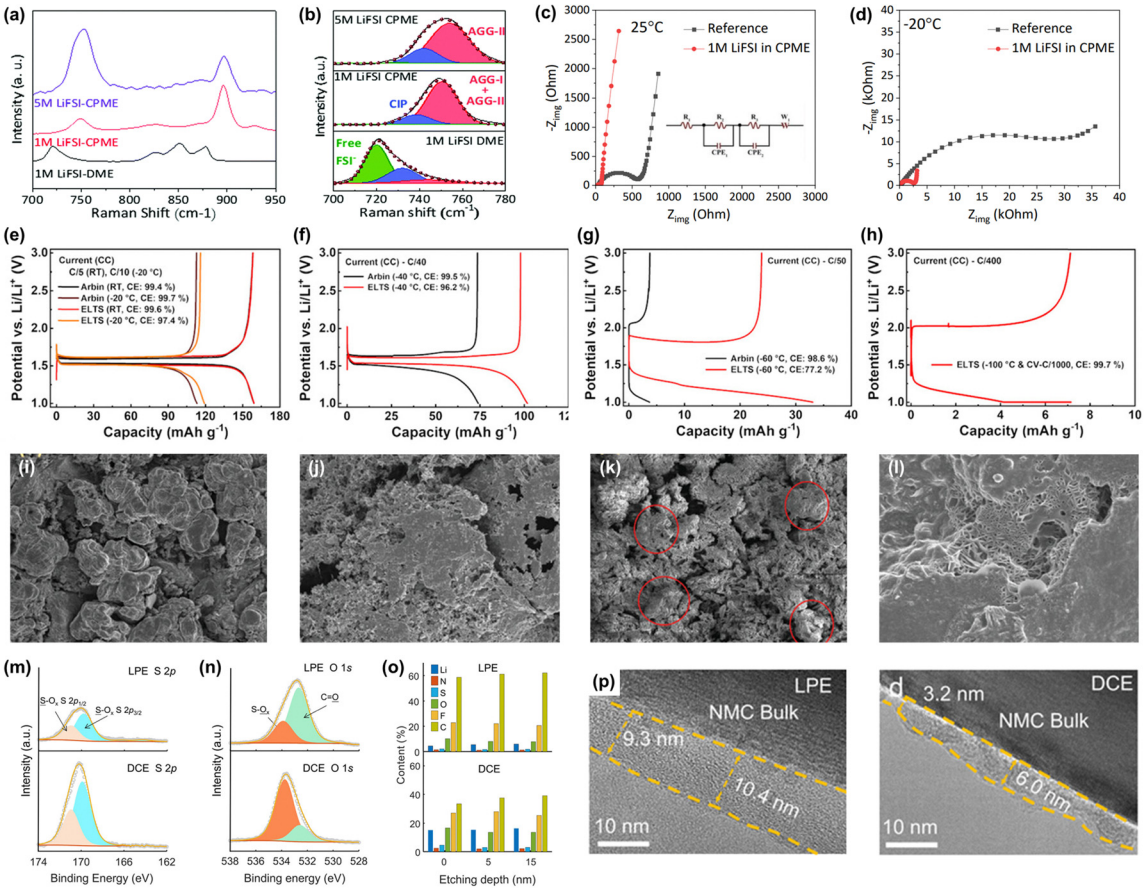

Fig. 1 (a) Raman spectra of electrolyte solutions composed of 1 M LiFSI in DME, 1 M LiFSI in CPME, and 5 M LiFSI in CPME. (b) Deconvoluted spectra of (a) for the spectrum range corresponding to FSI^- (700–780 cm^{-1}). EIS spectra measured for commercial electrolyte and 1 M LiFSI in CPME at (c) room temperature (25 °C) and (d) low temperature (−20 °C). Reproduced from ref. 11 with permission from the Royal Society of Chemistry. (e)–(h) Voltage profiles of Li‖LTO cells using 1 M LiFSI in CPME electrolyte solution was tested in both battery tester from Arbin Instruments and ELTS (e) at room temperature (C/5) and −20 °C (C/20), (f) −40 °C (C/40), and (g) −60 °C (C/50). (h) Voltage profiles of the cells having the same configuration, cycled using ELTS at −100 °C. Reproduced from ref. 12 with license under Creative Commons CC-BY 4.0. Scanning electron microscopy (SEM) images of anode and cathode morphology of Li–S pouch cells after the cycling test. Images of (i) Li metal anode and (j) S cathode of the 1.45 A h cell with low-sulfur loading, contrary to those of (k) Li metal anode and (l) S cathode of the 1 A h cell with high-sulfur loading. Reproduced from ref. 14 with license under Creative Commons CC-BY 4.0. XPS spectra of (m) S 2p and (n) O 1s for the cathodes using either low-polarity electrolyte (LPE, 1 M LiFSI in EMC/FEC/tetrafluoro-1-(2,2,2-trifluoroethoxy) ethane, 1.5 : 1.5 : 7 vol%) or decoordination electrolyte (DCE, 1 M LiFSI in EMC/FEC/DTF, 1.5 : 1.5 : 7 vol%) after cycling test. (o) The atomic ratio calculated from the XPS depth profiling for the cathodes in (m) and (n). High resolution-TEM images of CEIs using either (p) LPE or (q) DCE. Reproduced with permission from ref. 15. Copyright 2024 American Chemical Society.

structure of the Li–S battery.[14] This interaction reduced the solubility and mobility of polysulfides in the electrolyte, thereby mitigating their diffusion into the anode and ultimately leading to effective sulfur utilization and extended cycle life. It also lowered the Li^+ desolvation energy and enhanced ion transport at the electrode–electrolyte interface. Additionally, NO_3^- mitigated electrolyte decomposition at the lithium metal anode, formed a more stable SEI, and prevented excessive growth of lithium dendrite and dead lithium formation, which are major issues in low-temperature operation (Fig. 1i–l). As a result, 1.45 A h pouch cell achieved an initial discharge capacity of 584 mA h g^{-1}, which became 598 mA h g^{-1} after the 50th cycle, showing a Coulombic efficiency (CE) of 98.81% under −25 °C.

Moreover, other novel solvents showing distinct solvation dynamics were explored by a wide variety of studies in literature. Cui *et al.* applied a push–pull electrolyte design strategy using molecular electrostatic potential screening to enhance lithium metal battery (LMB) performance under high-voltage and low-temperature conditions.[15] This approach led to the identification of 2,2-difluoroethyl trifluoromethanesulfonate (DTF) as a cosolvent to control Li^+ solvation/desolvation kinetics. The sulfonyl moiety in DTF extracts Li^+ from solvent coordination, while the difluoromethyl group disrupts hydrogen bonding, thereby accelerating Li^+ transport. Furthermore, X-ray photoelectron spectroscopy (XPS) analyses revealed higher S 2p and O 1s signals of inorganic-rich CEIs (Fig. 1m–o), which prevents degradation and enhances electrochemical stability, as verified through high-resolution transmission electron microscope (TEM) measurements (Fig. 1p and q). Under −40 °C, Li‖$LiNi_{0.8}Co_{0.1}Mn_{0.1}O_2$ (NMC811) cells retained 93% of their capacity after 100 cycles and delivered 153 mA h g^{-1}. Zheng *et al.* developed a novel fluorinated solvent system and incorporated Na^+ as hetero-cation

additives to achieve stable LIB operation at −40 °C.[16] The introduction of multiple fluorine (–F) groups creates a strong electron-withdrawing effect, reducing their binding affinity with the charge carrier. The electrolyte formulation consisted of 1 M LiFSI in *trans*-4,5-di-fluoroethylene carbonate/methyl (2,2,2-trifluoroethyl) carbonate/hexafluoroisopropyl methyl ether (1 : 2 : 2 vol%) lowered Li^+ desolvation energy to 30.76 kJ mol^{-1}, promoting favorable charge transfer kinetics. Structural analysis revealed that Na^+ coordination modifies solvation structures, forming a Li–Na hybrid SEI enriched with LiF and NaF nanocrystals, which reduces interfacial resistance and prevents lithium plating. *Cryo*-TEM confirmed a compact, inorganic-rich SEI layer that improved lithium-ion transport and led to stable low-temperature cycling. Finally, graphite/$LiNi_{0.5}Co_{0.2}Mn_{0.3}O_2$ (NCM523) full cells generated 125 mA h g^{-1} at −20 °C, while 270 Wh kg^{-1} pouch cells retained 108.7 mA h g^{-1} at −40 °C for over 60 cycles. Through another work, Luo *et al.* developed a weak-solvation and low-viscosity electrolyte using isobutyronitrile (iBN) as a cosolvent to enable ultra-low temperature LIB operation down to −70 °C.[17] The electrolyte demonstrated high ionic conductivity (1.152 mS cm^{-1} at −70 °C) due to the reduced Li^+–solvent interaction, facilitating efficient desolvation and charge transfer kinetics. EIS and MD simulations confirmed that the weakened Li^+ solvation structure enabled faster Li^+ transport and reduced interfacial resistance. XPS and TEM analyses indicated that the electrolyte formed a thin and stable SEI, minimizing risk of Li plating at sub-zero temperatures. Galvanostatic cell cycling revealed that graphite‖$LiCoO_2$ full cells retained 75.8% of their room temperature capacity at −40 °C and 68.7% at −70 °C, significantly outperforming conventional carbonate-based electrolytes. Pouch cell testing validated stable cycling from −70 °C to 60 °C, supporting its practical applicability for large-area extreme-temperature batteries.

Similar to LIBs, extensive research was conducted on the solvation structures for SIBs to enhance their performance across a wide range of temperatures. Wang *et al.* demonstrated a novel temperature-responsive electrolyte design by adjusting solvent–solvent interactions, shifting the focus from conventional ion–solvent interactions.[18] The electrolyte was composed of sodium hexafluorophosphate ($NaPF_6$) dissolved in a solvent mixture of 2-methyltetrahydrofuran (MeTHF), tetrahydrofuran (THF), and anisole. Temperature-dependent interactions between anisole and the co-solvents played a key role in improving battery performance across a broad temperature range (−40 °C to 55 °C). In a similar study, Yang *et al.* combined strongly solvating diethylene glycol dimethyl ether (DIG) and weakly solvating THF with $NaPF_6$, enabling spontaneous solvation structure transformation at low temperatures to prevent salt precipitation.[19] This electrolyte design demonstrated remarkable performance in a hard carbon (HC)‖$Na_{2/3}Ni_{1/4}Cu_{1/12}Mn_{2/3}O_2$ full cell, achieving 90.6% capacity retention over 400 cycles at −40 °C.

2.2. Advanced electrolyte systems

2.2.1. Localized high-concentration electrolytes. Extended from the concept of solvation structure design, localized high-concentration electrolytes (LHCEs) have emerged as another viable solution to the challenges faced by LIBs and lithium–metal batteries (LMBs) in extremely low-temperature environments. LHCEs are strategically designed to retain the benefits of high-concentration electrolytes (HCEs) while minimizing their limitations. In HCEs, the strong solvation of Li^+ by anions leads to the formation of a stable SEI that enhances lithium metal compatibility. However, their high salt concentration drastically increases viscosity and lowers overall ionic mobility, limiting their practical applicability at low temperatures. LHCEs address these issues by incorporating non-solvating diluents that compensate high viscosity and promote ion transport without disrupting the localized solvation structure of Li^+. This unique solvation environment allows LHCEs to maintain anion-rich solvation shells, which facilitate the formation of an inorganic-rich SEI, known to improve lithium deposition uniformity and suppress dendrite growth. Moreover, LHCEs enable the use of low-freezing-point solvents that further expand the operational temperature of batteries, maintaining liquid-phase transport under temperatures as low as −60 °C.

Salt concentration within the electrolyte plays a pivotal role in the solvation kinetics of LHCEs. As concentration increases, several key changes occur in the solvation structure, including the reduction of free solvent molecules, leading to the formation of high-concentration coordination clusters and an increase in ion–ion interactions, ultimately resulting in the formation of CIPs and AGGs. Kim *et al.* developed an EC-free high salt concentration electrolyte (HSCE) using LiFSI in THF.[20] Unlike conventional carbonate electrolytes, which suffer from high viscosity, poor ion transport, and freezing at low temperatures, THF-based HSCE electrolytes enable efficient Li^+ transport *via* intra-aggregate ion exchange mechanisms. MD simulations articulated that at high salt concentrations, THF molecules are displaced by FSI^- anions, promoting labile anion exchange and solvent-independent SEI formation (Fig. 2a and b). The anion-derived LiF-rich SEI formed by HSCE provided boosted Li^+ diffusion, lower interfacial resistance, and enhanced interfacial stability. Cycling tests showed that graphite‖$LiNi_{0.6}Co_{0.2}Mn_{0.2}O_2$ (NCM622) full cells retained 80% of their room temperature capacity at −20 °C and 43% at −40 °C. In the following work, Kim *et al.* further implemented a THF-based LHCE to enable LMB operation at extreme low temperatures (−60 °C).[21] Based on the identical combination of LiFSI salt and THF solvent, the incorporation of 1,1,2,2-tetrafluoroethyl-2,2,3,3-tetrafluoropropyl ether (TTE) as a diluent made the electrolyte to maintain a stable liquid phase and ensure high ionic conductivity at low temperatures. The tailored solvation structure formed a Li_2O/LiF-rich SEI, improving lithium metal stability and prohibiting dendrite formation (Fig. 2c). Li‖NCM811 full cells retained 75% of their room temperature capacity at −20 °C and 64% at −40 °C, validating successful operation at –60 °C. It was verified that compared to conventional electrolyte system, new LHCE system accelerated lithium transport and suppressed interfacial side reactions, leading to higher CE and extended cycle life.

To further optimize the functionality of LHCE, solvent polarity engineering was adopted. By tuning the polarity of coordinating solvents by incorporating non-polar or weak polar

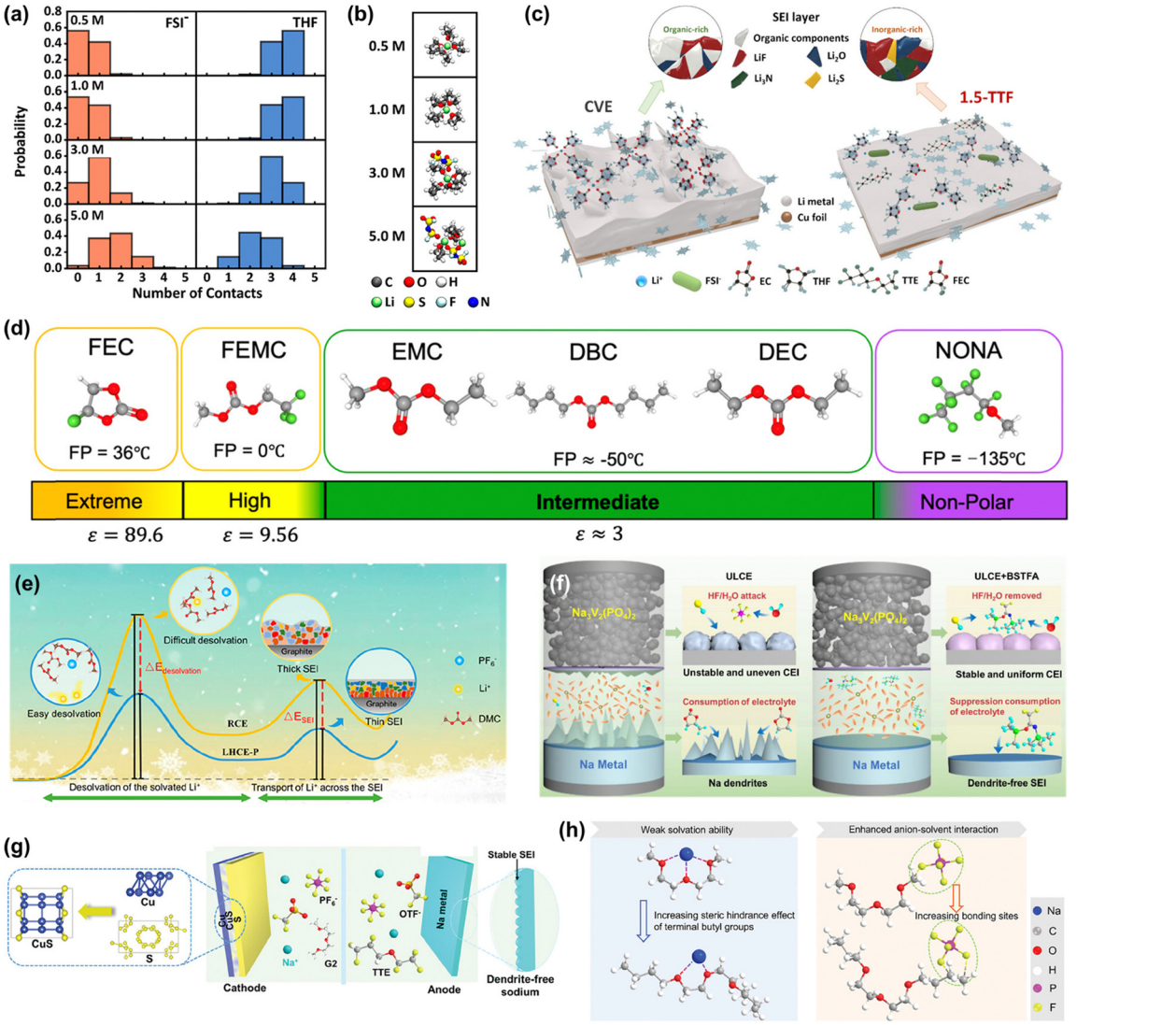

Fig. 2 (a) Histogram of the number of contacts between FSI^-–Li^+ and THF–Li^+ and (b) corresponding mode solvation structures of Li^+ in the first solvation shell depending on LiFSI concentration (0.5, 1.0, 3.0, and 5.0 M), calculated by MD simulation. Reproduced with permission from ref. 20. Copyright 2022 American Chemical Society. (c) Schematic illustration of Li^+ solvation and SEI chemistries based on the interactions between the Li metal anode and THF-based LHCE. Reproduced from ref. 21 with license under Creative Commons CC-BY 4.0. (d) Illustrative abstract of gradient LHCE employing stepwise polarity distribution. FP denotes freezing point. Reproduced from ref. 22 with license under Creative Commons CC-BY 4.0. (e) Schematic illustration displaying reduced desolvation energy and improved charge carrier transport attributed to LHCE-P, which denotes LHCE incorporating LiDFBOP as an additive. Reproduced with permission from ref. 25. Copyright 2023 American Chemical Society. (f) Schematic illustration demonstrating mechanism of preferential decomposition of BSTFA in the SMB. Reproduced with permission from ref. 30. Copyright 2021 Elsevier. (g) Schematic illustration of SMBs based on dual-salt electrolyte consisted of NaOTF, NaPF6 in DIG with TTE additives. Reproduced with permission from ref. 35. Copyright 2024 John Wiley and Sons. (h) Schematic illustration comparing the solvent–ion interaction of DIG with D2, inducing strong anion–solvent interactions. Reproduced with permission from ref. 37. Copyright 2025 John Wiley and Sons.

co-solvents, studies aim to balance ionic mobility, solvation dynamics, and electrolyte stability. One effective approach was to introduce gradient polarity electrolytes, where a stepwise reduction in solvent polarity refined solvent miscibility while maintaining robust Li^+ transport. Packard *et al.* introduced a gradient LHCE into LMBs to enhance low-temperature performance.[22] By inducing polarity slope with fluoroethylene carbonate (FEC) and nonafluorobutyl methyl ether (NONA), the electrolyte achieved ultra-low freezing points below −120 °C while maintaining high ionic conductivity. The following incorporation of methyl 2,2,2-triflooethyl carbonate (FEMC) with either diethylene carbonate (DEC), ethyl methyl carbonate, or dibutyl carbonate as an intermediate solvent further enhanced Li^+ mobility and electrolyte stability (Fig. 2d). In comparison with a three-solvent LHCE with 14% diluent incorporation (−85 °C freezing point), the new four-solvent gradient LHCE allowed 37.5% diluent incorporation, eventually leading to faster ion transport and stable SEI formation. LMBs using this electrolyte exhibited superior cycling performance, retaining 68% of their room temperature capacity at −50 °C (109.2 mA h g^{-1}

initial capacity at room temperature), significantly outperforming both three-solvent and commercial EC:DEC-based electrolytes. A similar work by Adams *et al.* formulated a novel ternary fluorinated electrolyte by combining lithium salts with two fluorinated polar carbonate solvents having high dielectric constant (FEC, ε = 110) and lower dielectric constant (FEMC, ε = 9.56) to achieve an ultra-low freezing point while maintaining high ionic conductivity.[23] To maintain the desired solvation structure, this mixture was then strategically diluted with a weakly polar NONA, which also has an extremely low freezing point of −135 °C, to formulate the final electrolyte composition (denoted as F-FFN). Compared to a control electrolyte condition, which failed at −25 °C, F-FFN retained 61% at −50 °C compared to its room temperature capacity. EIS analysis revealed that F-FFN exhibited a lower charge transfer activation energy (55.71 kJ mol^{-1}), indicating a higher Li^+ transport capability, attributed to its tailored solvation structure, which has a higher fraction of lithium salt anions. XPS measurement confirmed the formation of a LiF-rich CEI, further stabilizing low-temperature cycling. Furthermore, Li *et al.* explored non-polar ether-based electrolytes to minimize the solvation strength of Li^+, thereby facilitating charge transfer kinetics and enhancing electrolyte compatibility with high-voltage cathodes.[24] By using a dipropyl ether (DPE)-based electrolyte with LiFSI salt, the study demonstrated improved electrochemical stability and suppressed side reactions. The low polarity of electrolytes and weak Li^+ solvation generated a robust CEI, preventing electrolyte decomposition at high voltages. When tested with Li‖NCM811 configuration, the cells using DPE electrolyte exhibited 74% capacity retention after 150 cycles at 25 °C, also exhibiting wide temperature capability. Notably, unlike conventional ether-based electrolytes, which suffer from anodic instability, the selective decomposition mechanism of LiFSI-derived anions ensured stable cycling up to 4.3 V.

A $LiPF_6$-based LHCE designed by Song *et al.* offered a significant breakthrough in improving the low-temperature performance of LIBs.[25] Such novel electrolyte was prepared by eliminating EC, increasing $LiPF_6$ concentration, and incorporating lithium difluorobis(oxalato)phosphate (LiDFBOP) as an additive in dimethyl carbonate (DMC). The electrolyte formulation optimizes Li^+ desolvation kinetics by forming a Li^+–solvent–PF_6^- complex, which reduces desolvation energy and improves charge transfer at sub-zero temperatures (Fig. 2e). EIS analysis confirmed that LiDFBOP led to the formation of a LiF-rich SEI layer, which lowers interfacial resistance and enhances cycling stability. The cycling tests on Li‖graphite half-cells revealed 240 mA h g^{-1} at −20 °C for the rate of 0.1C, exceeding the performance of commercial electrolyte. Pouch cells employing graphite‖NMC622 electrodes further validated superior rate performance and stable cycling at −20 °C, demonstrating the feasibility of LHCE for practical application. Holoubek *et al.* investigated the role of ion-pairing in electrolytes to enhance the low-temperature performance of LMBs.[26] By exploiting 1,2-dimethoxyethane (DME) as the solvating solvent and bis(2,2,2 trifluoroethyl)ether (BTFE) as a diluent, the solvation structure of Li^+ was systematically modulated, elucidating that increased ion-pairing with anions (FSI^-) reduced R_{ct} and improved lithium plating reversibility. EIS corroborated that higher local salt concentration increased Li^+ coordination with anions, enhancing interfacial charge transfer while maintaining oxidative stability and enabling stable cycling of 4.4 V full cells at −40 °C. MD simulations further validated that a moderate DME/Li^+ ratio is required for the electrolyte to transition to an anion-dominated solvation sheath, improving lithium metal reversibility at sub-zero temperatures. It was found that heavily ion-paired electrolytes, particularly those having a BTFE : DME ratio of 3 : 1, showed a significant leap on CE to become 98.9%, 98.5%, and 96.9% at −20, −40, and −60 °C, respectively, for Li‖Cu half-cells. Chen *et al.* proposed an anion-dominated conventional-concentration electrolyte (ACCE) to overcome the limitations of HCEs and LHCEs, such as high viscosity and salt precipitation at low temperatures.[27] By introducing lithium difluorophosphate ($LiPO_2F_2$) into a 1 M LiTFSI DMC/FEC/methyl acetate (MA) electrolyte, researchers engineered a dual-anion solvation mechanism, reducing Li^+–solvent interactions and lowering desolvation energy barriers. As a result, the electrolyte maintains high ionic conductivity (1.3 mS cm^{-1} at −50 °C), ensuring efficient charge transfer. It was also revealed that $PO_2F_2^-$ preferentially integrated into the Li^+ solvation sheath to form a LiF- and $Li_xPO_yF_z$-rich interphase, suppress solvent coordination, and stabilize the CEI. As a result, 0.75 A h graphite‖NCM811 full cells retained 72% of their capacity at −40 °C while demonstrating fast-charging capability at 6C under room temperature. Lin *et al.* developed a dual-salt LHCE using sulfolane and ethyl acetate (EA) with LiTFSI and lithium difluoro(oxalato)borate salts, optimized with 10 wt% FEC.[28] The electrolyte remained as liquid under −80 °C, demonstrating excellent ionic conductivity and fast charging/discharging capacity. EIS and MD simulations confirmed that the dual-salt system reduced Li^+ desolvation energy and stabilizes the interphase, developing a LiF- and boron-rich CEI layer, to function as a protection layer on the cathode. Li‖NCM523 full cells revealed 89% capacity retention after 200 cycles at 4.6 V and 1C (200 mA g^{-1}) at 25 °C, while at −40 °C, the battery retained 75% of its room temperature capacity and maintained stability over 200 cycles.

2.2.2. Ultra-low concentration electrolytes. Low-concentration electrolytes create a solvent-rich environment with abundant free solvent molecules, forming solvent-separated ion pairs (SSIPs) that reduce viscosity and enhance ion mobility. Li *et al.* proposed an electrolyte with a low concentration of 0.3 M $NaPF_6$ in EC/PC (1 : 1 vol%) for low-temperature SIBs.[29] The diluted electrolyte offered benefits such as low viscosity and wide operational temperature, ranging from −30 °C to 55 °C. A similar study by Jiang *et al.* introduced an acetamide additive, *N*,*O*-bis(trimethylsilyl)trifluoroacetamide (BSTFA) into ultra-low concentration electrolytes to enhance the performance of sodium metal batteries (SMBs) by scavenging H_2O and HF while inhibiting $NaPF_6$ decomposition (Fig. 2f).[30] The preferential decomposition of BSTFA at both electrodes formed organic- and NaF-rich interfacial layers, improving the stability and electrochemical performance of Na‖$Na_3V_2(PO_4)_3$ (NVP) cells under temperature from −18 °C to 55 °C. Another study by Feng *et al.* implemented 0.5 M $NaPF_6$ in DIG to develop a stable, amorphous, and monolithic electrolyte–electrode interphase for

SIBs, enabling superior ion transport in sub-zero environments.[31] Thin, stable, and organic-rich SEI/CEI layers were formed, which showed higher ionic conductivity and long-term stability, further impacting rate and cycling performance. This resulted in remarkable electrochemical performance at −30 °C, in that Na‖$Na_{0.7}Li_{0.03}Mg_{0.03}Ni_{0.27}Mn_{0.6}Ti_{0.07}O_2$ (LMNM'T) cells demonstrated superior discharge capacity, and rate capability, while Na‖HC half-cells provided a capacity of over 310 mA h g^{-1}.

2.2.3. Weakly solvating and high-entropy electrolytes. Despite their benefits in operational stability and safety, HCEs and LHCEs face challenges for widespread adoption, including increased viscosity, reduced ionic conductivity, and higher manufacturing process and cost.[32] Weakly solvating electrolytes (WSEs) present a promising alternative to HCEs and LHCEs, enabling precise control in anion solvation dynamics and SEI composition in dilute electrolytes. Fang *et al.* developed WSE by incorporating MeTHF into THF, to reduce Na^+–dipole interactions and promote anionic coordination in the first solvation sheath, ultimately leading to the formation of inorganic-rich SEI on HC anodes.[33] This novel electrolyte design enabled exceptional low-temperature performance, with HC‖NVP full cell retaining a high capacity of ∼100% after 250 cycles at −40 °C. Zhou *et al.* showed that incorporating a weak Na^+ solvating co-solvent (THF/DME) in the electrolyte enhances desolvation kinetics and enables high-rate performance in low-temperature SMBs.[34] This approach would form a NaF-rich SEI that suppresses dendrite growth and ensures stable cycling down to −60 °C. Similarly, a dual-salt electrolyte with WSEs creates an anion-rich solvation structure that can further refine solvation kinetics and form a stable interphase. For instance, a work reported by Yu *et al.* developed a dual-salt WSE composed of 0.25 M sodium trifluoromethanesulfonate (NaOTF) and 0.25 M $NaPF_6$ in DIG with TTE additive.[35] This method formed a protective NaF-rich SEI and enhanced the reversibility of sodium plating/stripping, thereby preventing excessive dendrite growth (Fig. 2g). It enabled the low-temperature performance of SMBs by achieving a reversible capacity of 202.8 mA h g^{-1} at −20 °C (1C) and 230.0 mA h g^{-1} at −40 °C (0.2C). Thenuwara *et al.* developed a dual-salt electrolyte combining sodium triflate and sodium tetrafluoroborate in DIG to induce sodium metal cycling with high CE at temperatures as low as −40 °C, maintaining an impressive ionic conductivity of 0.8 mS cm^{-1}.[36] The remarkable low-temperature performance is attributed to the formation of a uniform, inorganic-rich SEI, as revealed by cryogenic TEM and XPS investigations.

Recently, high-entropy electrolytes (HEEs) with high boiling points and low freezing points have become prospective candidates for wide-temperature and high-voltage rechargeable batteries. HEEs simultaneously promote the formation of stable SEI/CEI on the anode/cathode, respectively. Li *et al.* developed high-voltage anode-free sodium batteries (AFSBs) by designing an electrolyte based on the concept of sole-solvent HEE, with the combination of diethylene glycol dibutyl ether (D2) and $NaPF_6$ salt.[37] Unlike traditional multi-solvent systems, the single solvent approach simplifies formulation while leveraging unique solvent–ion interactions. D2 exhibited weak cation solvation but strong anion–solvent interactions, which derived entropy-enhanced salt dissociation and produced a high concentration of CIPs (Fig. 2h). MD simulations, Raman spectroscopy, and nuclear magnetic resonance analysis confirmed that these interactions led to the formation of robust, anion-derived interphases on both SEI and CEI. The developed AFSB pouch cell demonstrated impressive performance in a wide temperature range from −20 to 60 °C, achieving a high cell-level energy density of 209 W h kg^{-1} and maintaining 83.1% capacity retention after 100 cycles at 25 °C.

2.3. Interphase modulation

Interphase modulation primarily focuses on modifying the properties at the electrode–electrolyte interphase by forming a temperature-dependent layer. This approach mainly involves tailoring/engineering the SEI and CEI, passivation layers that form on respective electrode surfaces during operation. The most crucial factors influencing the interphase would be the electrolyte composition and the electrode material properties. The selection of solvents and conductive salts can tailor solvation dynamics, thereby affecting the structural and chemical properties of the interphases. The intrinsic properties of electrode materials, including their surface chemistry and morphological features, largely affect the development and stability of interphase layers. This holistic approach, considering both components of electrolyte and electrode, is essential for optimizing the performance and durability of electrochemical systems across diverse operating conditions.

Liu *et al.* formed a temperature-responsive SEI on sodium metal anode by combining fluorinated carbonates and antifreeze fluorobenzene (Fig. 3a).[38] This electrolyte design enabled the formation of a thin, organic-rich SEI at low temperatures to facilitate Na^+ ion diffusion (Fig. 3b–d). On the other hand, at high temperatures, it created a thick, inorganic-dominated SEI that inhibits parasitic reactions (Fig. 3e–g), allowing Na‖NVP cells to operate effectively across a broad temperature range from −20 °C to 60 °C. Liang *et al.* modulated the SEI/CEI layer by using phosphorus/silicon intermediates from additives in carbonate-based electrolytes to make SIB operable at a wide temperature range from −25 °C to 75 °C.[39] The optimized electrolyte consisted of PC as the main solvent with FEC and tris(trimethylsilyl) phosphite (TMSPi) as an additive, abbreviated as NPFT. NPFT-based full cells using NVPF cathodes and HC anodes demonstrated excellent stability for both low and high temperatures, retaining 93% capacity after 1000 cycles at 50 °C and delivering a good reversible capacity of 107 mA h g^{-1} at –25 °C. A similar study by Li *et al.* proposed a novel interphase enhancement mechanism using a sulfur-rich strategy, incorporating diethyl sulfite and dimethyl sulfite as co-solvents in a carbonate-based electrolyte to create a modified interface.[40] This strategy improved the SIB performance across a wide temperature range from −25 to 60 °C, demonstrating high-capacity retention of 87.7% at –25 °C and 88.2% at 60 °C after 100 cycles with HC‖NVP full cells.

2.4. Polymer and quasi-solid-state electrolytes

Polymer and quasi-solid-state electrolytes have emerged as potential solutions to overcome the critical challenges of liquid

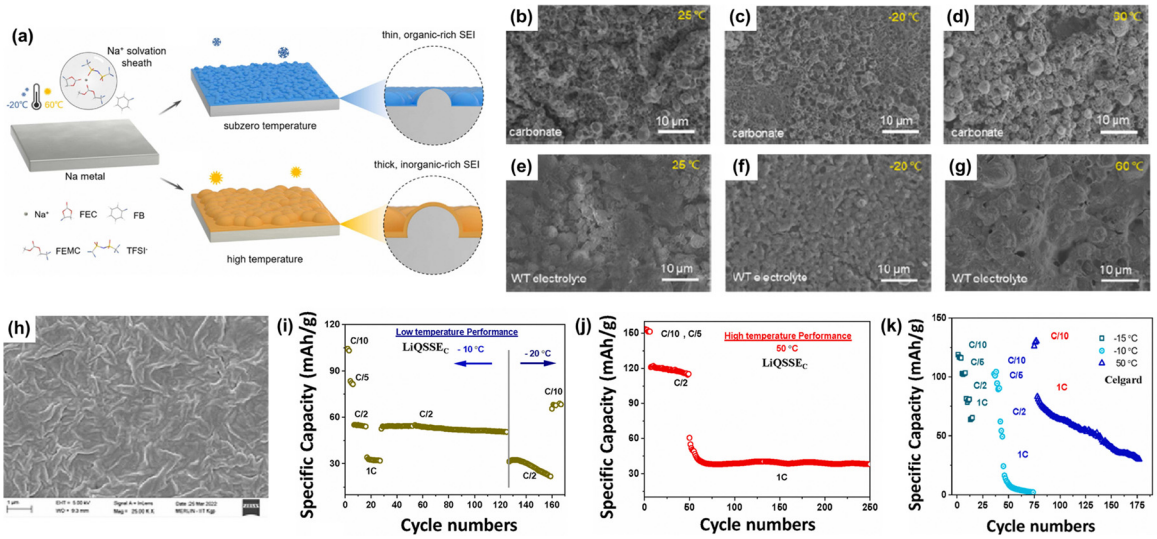

Fig. 3 (a) Schematic illustration of the formation of temperature-responsive SEI at sub-zero and high temperatures. Deposition of small Na deposits forms a thin, organic SEI at low temperatures, whereas larger Na deposits form a thick, inorganic SEI at high temperatures. SEM images of Na metal anode after the Na deposition. Images of the top surface morphology using conventional carbonate electrolyte under (b) 25 °C, (c) −20 °C, and (d) 60 °C, and wide-temperature (WT) electrolyte under (e) 25 °C, (f) −20 °C, and (g) 60 °C. Reproduced with permission from ref. 38. Copyright 2022 Elsevier. (h) Top-view SEM image of nonwoven coated with PVDF–HFP polymer. Cycling stability test results of Li‖LFP half-cell using nonwoven gel-based polymer electrolyte (LiQSSE) under (i) −10 °C and −20 °C, and (j) 50 °C at different C-rates. The temperature-dependent testing was conducted on the Li‖LFP half-cell using commercial Celgard separator under (k) −15 °C and −10 °C, and 50 °C at different C-rates. Reproduced with permission from ref. 41. Copyright 2024 Elsevier.

electrolytes, enabling wide-temperature operation while maintaining safety and performance. These quasi-solid-state electrolytes enhance Li^+/Na^+ ion transport by mitigating dendrite growth. Nonetheless, these electrolytes suffer from lower conductivity in the bulk and poor electrode–electrolyte interfacial contacts, which limits their practical implementations, leaving room for future development.

Das *et al.* reported LIBs fabricated with a novel, nonflammable, flexible, quasi-solid-state polymer electrolyte operated under −20 °C to 50 °C.[41] This nonwoven fabric-supported electrolyte composed of methyl propionate (MP), trimethyl phosphate (TMP), FEC, and poly(vinylidene fluoride-*co*-hexafluoropropylene) (PVDF–HFP) polymer demonstrated superior thermal stability and nonflammability (Fig. 3h). The quasi-solid-state polymer matrix facilitated uniform Li^+ transport, reduced polarization, and prevented dendrite growth, which are all beneficial features for low-temperature operation. A low-temperature cycling test at −20 °C demonstrated that a Li‖LFP half-cell exhibited a specific capacity of 68 mA h g^{-1} and 31 mA h g^{-1} at a rate C/10 and C/2, respectively (Fig. 3i–k). Notably, at −10 °C, the cell achieved stable cycling at C/2, retaining 93% with an initial capacity of 54 mA h g^{-1} (Fig. 3i). The full-cell configuration having LFP/graphite exhibited an initial discharge capacity of 115 mA h g^{-1} at C/10, with 57% capacity retention after 100 cycles. Moreover, the electrolyte also exhibited low heat release (37 J g^{-1}) compared to commercial liquid electrolytes (1.5 kJ g^{-1}), improving thermal stability and widening operation temperature.

He *et al.* obtained an excellent fast-charging performance in LMBs by *in situ* formation of quasi-solid-state polymer electrolyte.[42] The electrolyte was prepared by *in situ* polymerization of polyethylene glycol monomers in low-melting solvent (1,3-dioxolane), demonstrating exceptional ionic conductivity and electrochemical performance under the temperature from −20 °C to 60 °C. A similar study by Li *et al.* developed a quasi-solid-state polymer electrolyte through *in situ* polymerization using a 1,3,5-trioxane-based precursor.[43] The electrolyte formed a dual-layered SEI on the Li metal electrode, enabling a stable operation of Li‖$LiNi_{0.8}Co_{0.1}Mn_{0.1}O_2$ half-cells at temperatures as low as −30 °C. Yu *et al.* reported an *in situ* polymerized conductive quasi-solid-state polymer electrolyte for high-voltage and low-temperature application, with excellent lithium metal compatibility and long-term stability.[44] Li‖$LiFePO_4$ full cell achieved 89% capacity retention after 2000 cycles at 1C at room temperature, while Li‖NMC811 cell exhibited stable low-temperature performance, delivering discharge capacities of 77 mA h g^{-1} at −20 °C and 64 mA h g^{-1} at −30 °C and during cycling tests. Therefore, recent advancements in polymer and quasi-solid-state polymer electrolytes delivered an excellent performance and stability across a wide temperature range, paving a way for more versatile and efficient energy storage capable of operating in extreme conditions.

3. Electrode engineering

The performance of LIBs and SIBs at low temperatures is primarily influenced by the cathode and anode. As ion exchange is occurring, the cathode determines the ion transport properties, structural stability, electrochemical reversibility, and storage capacity of the battery. Low temperatures lead to a reduced

ion diffusion coefficient and increased R_{ct}, which causes significant polarization and impairs the (de)lithiation process, resulting in energy and capacity loss. Similarly, on the anode side, sub-zero temperatures exacerbate poor electronic and ionic conductivity, affected by sluggish ion diffusion and restricted desolvation kinetics. More critically, Li/Na plating and dendrite formation pose serious safety and stability concerns. Since anode (de)intercalation kinetics is a dominant factor in battery performance, optimizing anode design is also crucial. To address these challenges, various electrode modifications have been explored, including the introduction of novel electrode materials, supplementation of structural imperfections, surface and interface treatments, and modification of morphological properties. Recent innovations in electrode design emphasize the significant potential of structurally tailored materials in overcoming limitations under low-temperature conditions and mitigating safety issues.

3.1. Multicomponent electrode materials

Novel designs of multicomponent electrodes have strategically employed heterogeneous structure, hybrid composites, and (metallic) alloy to boost Li^+ diffusion and enhance Li^+ desolvation ability to improve overall electrochemical performance.[45] Kim *et al.* developed an amorphous multiple-anionic transition metal compound electrode, enabling an ultra-wide operational window ranging from −100 °C to 45 °C.[46] The proposed iron hydroxyl selenide (Fe(OH)Se) anode, when paired with the aforementioned CPME-based electrolyte, facilitates efficient Li^+ conduction at extreme temperatures. XPS measurement confirmed that Fe(OH)Se forms a $Fe(OH)_x/FeSe_y$ heterostructure during cycling (Fig. 4a–c), which enhances ion diffusion pathways and conversion reaction kinetics at low temperatures. The CPME electrolyte, with its low viscosity and suppressed freezing point, ensured continuous ion conduction at sub-zero temperatures while stabilizing the LiOH/Li_2Se-rich SEI, which suppressed side reactions and interfacial degradation. The cycling test demonstrated that Li‖Fe(OH)Se cells delivered 285.2 mA h g^{-1} at −80 °C and showed exceptional operability at −100 °C, while retaining 974.7 mA h g^{-1} at room temperature and 1066.9 mA h g^{-1} at 45 °C. Another study by Koppisetti *et al.* incorporated LiF to synthesize biphasic cathode material ($Na_{0.67}Li_{0.07}Mn_{0.5}Co_{0.5}O_{2-x}F_x$).[47] This attempt demonstrated superior energy output and structural stability compared to single-phase sodium oxide material ($Na_{0.67}Mn_{0.5}Co_{0.5}O_2$) in conventional SIBs. The integration of LiF in the synthesis of biphasic cathode materials reduced structural distortion and enhanced Na^+ kinetics and Na storage, resulting in excellent capacity retention of 85% after 100 cycles (0.2C) at room temperature and 94% at −20 °C after 100 cycles (0.1C). Chen *et al.* reported sodium superionic conductor-type $Na_4Fe_3(PO_4)_2(P_2O_7)$/C nanocomposite as a cathode material of SIBs for all-climate applications (Fig. 4d).[48] As verified through the density functional theory (DFT) and bond valence sum (BVS) calculations, $Na_4Fe_3(PO_4)_2P_2O_7$ possesses unprecedented 3D sodium diffusion pathways due to a mixed crystalline structure (Fig. 4e), which led to long-term cyclability and low-temperature performance. The following cell test achieved specific capacities of 95.0 mA h g^{-1} and 84.7 mA h g^{-1} at 0.1C and 0.2C, respectively at −20 °C. The cells also exhibited outstanding cycling performance across a wide temperature range, retaining 92.1% at −20 °C and 91.4% at 50 °C.

Other studies innovated the anodes by replacing conventional HC into 3D hierarchical hetero-nanostructure composites. Pure HCs are known to have low working voltage and form sodium dendrite at high current densities. To resolve these issues, Zhao *et al.* selected $NaTi_2(PO_4)_3$ (NTP) as an anode and $Na_{2.4}Fe_{1.8}(SO_4)_3$ cathode.[49] Together with ester-based electrolyte, SIBs exhibited remarkable cycling stability with 70.7% capacity retention after remarkable 10 000 cycles at a 10C rate, showing reliable operation across a wide temperature range from –50 °C to 90 °C. Another study by Li *et al.* adopted a combination of Bi anode, carbon-coated $Na_4Fe_3(PO_4)_2P_2O_7$ (NFPP@C) cathode, and DIG-based electrolyte to enable a remarkable temperature range from −70 to 100 °C.[50] The working principles were the solvent co-intercalation in Bi anode and high Na^+ diffusion coefficient of NFPP@C cathode, assisted with a low freezing point of the electrolyte. A similar work by Wang *et al.* showcased a high-performance SIBs using a bulk Bi anode, NVP/carbon nanotubes composite (NVP-CNTs) cathode, and $NaPF_6$-DIG electrolyte, achieving power density of 2354.6 W kg^{-1} and energy density of 150 W h kg^{-1}, with superior cycling stability from −15 °C to 45 °C.[51] Lastly, Tian *et al.* employed 3D hierarchical $FeSe_2$/rGO hetero-nanostructure hybrid anode for low-temperature operations.[52] The rGO membrane formed a network with $FeSe_2$ nanoparticles embedded in nests. This structure provides fast transport channels for Na^+, alleviating volume expansion during charge/discharge cycles and accelerating reaction kinetics. The $FeSe_2$/rGO anode displayed remarkable temperature adaptability, maintaining superb capacity retention of 53.1% at −40 °C and 82.1% at 60 °C.

The alloying process involves integration of metallic elements, such as Sb, Pb, and Bi, into anode materials to improve electronic conductivity, while mitigating volume expansion. For instance, Varzi *et al.* designed 3D porous Cu–Zn alloy anodes to overcome the limitations of conventional Zn-based anodes (Fig. 4f and g).[53] The alloy fabricated *via* the dynamic hydrogen bubble template (DHBT) method exhibiting high electronic conductivity, structural stability, and fast Li^+ transport pathways, enabling superior electrochemical performance at sub-zero environment (Fig. 4h). The porous architecture reduced R_{ct} and promoted rapid Li^+ diffusion, offering efficient lithiation/delithiation kinetics under extreme cold. Both *in situ* and *ex situ* XRD results further revealed a reversible Zn displacement mechanism, preventing electrode degradation. Final cell tests showed that $Cu_{18}Zn_{82}$ retained 200 mA h g^{-1} at −20 °C, whereas conventional graphite anodes suffered a drastic capacity drop to 12 mA h g^{-1}.

3.2. Structural design

Structural imperfections such as defects, vacancies, dislocations, and grain boundaries significantly influence ion diffusion and, consequently, the intrinsic conductivity of electrode materials. For instance, disordered carbon materials for sodium storage and metal deposition can be improved through various

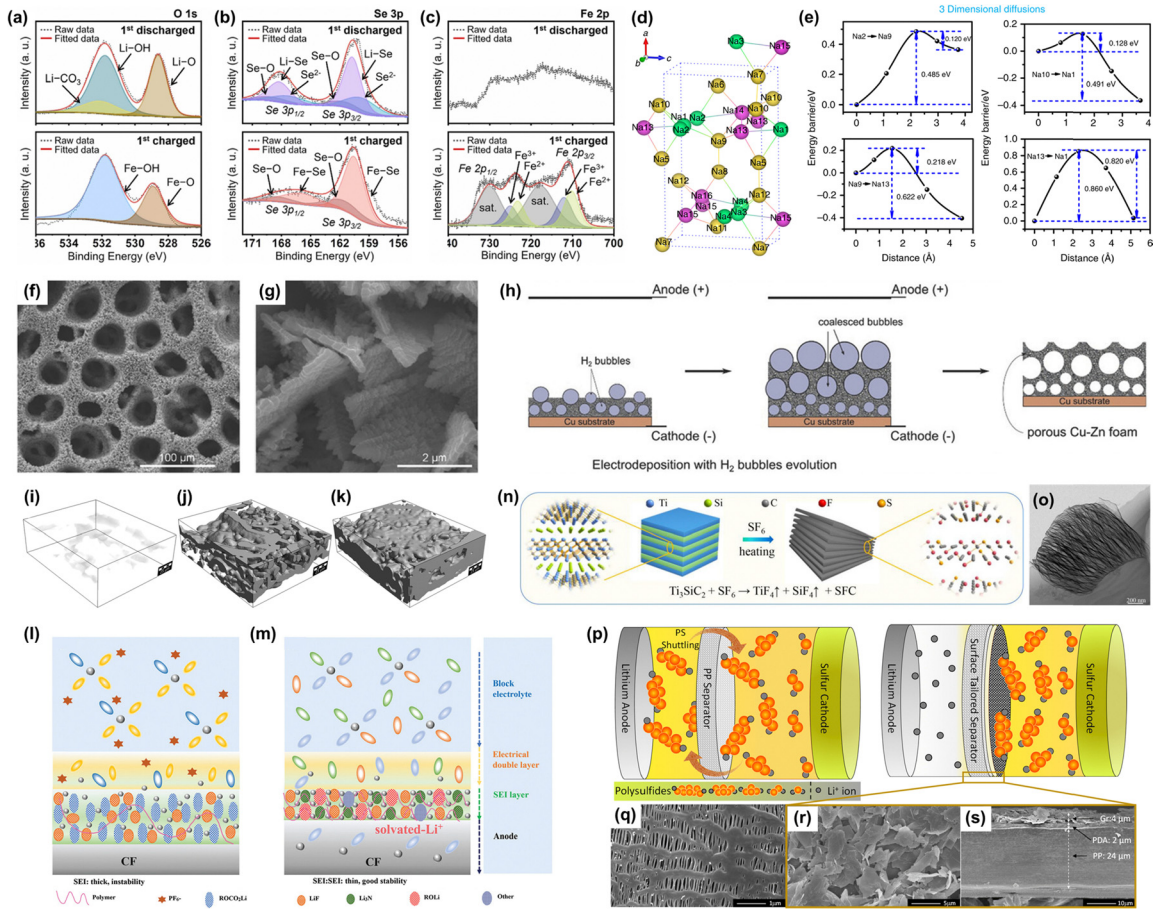

Fig. 4 XPS spectra of (a) O 1s, (b) Se 3p, and (c) Fe 2p for Fe(OH)Se anode using 1 M LiFSI in CPME as an electrolyte after the first discharge and charge cycles. The delithiation of Fe(OH)Se produced $Fe(OH)_x$ and $FeSe_y$, indicating the formation of heterostructure compounds. Reproduced with permission from ref. 46. Copyright 2024 Elsevier. (d) The crystal structure of $Na_4Fe_3(PO_4)_2(P_2O_7)$ depending on the types of Na^+ sites and (e) the energy barrier diagrams for the migration between different Na^+ ion groups. Reproduced from ref. 48 with license under Creative Commons CC-BY 4.0. (f) and (g) Top-view SEM images of porous $Cu_{20}Zn_{80}$. (h) Schematic illustration of the DHBT process, depicting the dynamic templating of bubbles, which displaces the surrounding solution and alters the morphology of the metallic deposit. Reproduced with permission from ref. 53. Copyright 2017 John Wiley and Sons. 3D X-ray microtomography imaging for the distribution of non-carbonaceous species in electrode (i) without plating, (j) after 10 cycles of plating, and (k) after 20 cycles of plating. Reproduced with permission from ref. 54. Copyright 2024 Elsevier. Schematic illustration of the SEI layer formed by the electrolyte with (l) $LiFP_6$–EC–EMC–VC and (m) LiFSI–THF–LNO. Reproduced with permission from ref. 56. Copyright 2024 John Wiley and Sons. (n) Schematic illustration of the synthesis of SFC and (o) TEM image displaying its accordion-like structure. Reproduced with permission from ref. 57. Copyright 2022 Elsevier. (p) Schematic illustration describing suppressed polysulfide diffusion within the Li–S cell with graphene-PDA-coated separator, compared to the cell using PP separator that demonstrates polysulfide shuttling. SEM images of (q) top surface of pristine PP separator and (r) graphene-PDA-coated separator, and (s) cross-section of graphene-PDA-coated separator. Reproduced with permission from ref. 59. Copyright 2022 Royal Society of Chemistry.

strategies, including interlayer spacing widening, heteroatom doping, porous structures, surface functional groups, composite formation, and modified electrolyte composition.

Yadav *et al.* adopted an advanced microstructure having properties such as larger interlayer spacing, partial graphitization, high mesoporosity, and N-doping to emphasize their role in sodium plating/stripping processes for improved sodium storage.[54] Through XPS and X-ray microtomography, it was confirmed that these features boosted charge transfer, refined diffusion properties, and stimulated the formation of a stable SEI (Fig. 4i–k). The study highlighted the use of sodiophilic N-doped polymer-derived carbon (PDC) as an effective anode material for both SIBs and SMBs. Combined with $Na_3V_2(PO_4)_2F_3$ cathodes, PDC delivered a capacity of 173 mA h g^{-1} at 1 A g^{-1} in half-cells and 84 mA h g^{-1} at 1C in full cells. Such modification enabled efficient Na^+ storage from −20 °C to 50 °C and ensured high cycling stability with a CE of 99.45% over 1000 cycles. To the best of our knowledge, this study represents the first successful demonstration of sustainable carbon-based materials achieving such an expansive temperature range for sodium storage.

Introducing oxygen vacancies through controlled calcination in a reducing atmosphere has shown to enhance ionic and electronic conductivity. Jiang *et al.* developed a partially reduced $TiNb_{24}O_{62}$ (PR-TNO) anode, exploiting its expanded interlayer spacing (0.3835 nm) and high electronic conductivity (7.8×10^{-5} S cm^{-1}, three orders of magnitude higher than untreated TNO).[55] The ReO_3-type layered crystal structure of PR-TNO enabled fast Li^+ transport and notable capacitive behavior,

ensuring stable operation at sub-zero temperatures. EIS and *in situ* XRD/TEM analyses confirmed that the low activation barrier for Li^+ diffusion and stable structural integrity contributed to superior performance. XPS and TEM studies revealed a thin SEI ($\sim$1.0 nm at -20 °C) composed of LiF-rich compounds, minimizing interfacial resistance. The cycling test revealed that PR-TNO retained 83.3% of its room temperature capacity at -20 °C (313 mA h g^{-1} at 0.1C) and exhibited a high-rate capability (58.3% retention at 5C *vs.* 0.5C). Furthermore, pouch cell testing validated a stable operation over 1680 cycles with 99.2% capacity retention, implying its scalability potential.

3.3. Interfacial engineering

Interfacial engineering enhances the functionality of electrodes in low-temperature LIBs/SIBs by optimizing the electrode–electrolyte interface to facilitate efficient ion transport and reduce interfacial resistance. This approach involves strategies such as surface coating, electrode configuration optimization, and interfacial chemistry control, thereby advancing charge transfer kinetics and overall battery efficiency under sub-zero conditions.

A hybrid LMB with optimized interfacial chemistry was developed by Lyu *et al.*, addressing the trade-off between energy density and cycle life.[56] By integrating a lithiophilic carbon film (CF) anode, lithium metal consumption was minimized while maintaining high CE at low N/P ratios. Through testing a series of Li salts, 1 M LiFSI–THF with 0.5 wt% $LiNO_3$ (LiFSI–THF–LNO) was identified as the most effective, offering a high Li intercalation capacity of 236.5 mA h g^{-1}, along with upgraded rate capability and cycling stability. Structural analysis and MD simulations revealed that Li_3N-enriched SEI formed by $LiNO_3$ decomposition significantly lowered interfacial resistance, facilitating fast charge transfer under low temperatures. It was elucidated that LiFSI–THF–LNO electrolyte formed an elastic, inorganic-rich SEI that enhances Li^+ diffusion, plating/stripping uniformity, and cycling stability at room and low temperatures, whereas $LiPF_6$–EC–EMC–VC electrolyte exhibited slow desolvation and uneven SEI that promoted Li dendrite growth, especially at low temperatures (Fig. 4l and m). As a result, CF‖NCM811 full cells exhibited 527.3 mA h g^{-1} at 25 °C and 381.5 mA h g^{-1} at -20 °C, achieving energy densities of 312.6 and 223.7 W h kg^{-1}, respectively. Moreover, a 100 mA h-level pouch cell exhibited 83% capacity retention over 500 cycles, verifying long-term stability.

3.4. Morphology control

Morphological control strategies, including the design of nanoparticles, nanowires, nanosheets, and complex nanostructures, enhance low-temperature performance by shortening Li^+ diffusion paths, reducing electrode polarization, and increasing electrode surface area, thereby improving electrochemical kinetics overall.

Wang *et al.* developed an accordion-like S/F co-doped carbon (SFC) anode to obtain superior low-temperature performance of LMB.[57] The SFC electrode, synthesized *via* etching Ti_3SiC_2 in an SF_6-containing atmosphere (Fig. 4n and o), exhibited higher lithiophilicity and formed a Li_2S–LiF-rich SEI, stabilizing the interface and suppressing dendrite growth. DFT calculations confirmed that the strong interaction between Li and S/F-doped carbon significantly reduced Li nucleation barriers, facilitating uniform Li deposition. EIS and XPS analyses validated the role of the electrolyte in maintaining low interfacial resistance and stable lithium plating/stripping cycles. Galvanostatic cycling tests demonstrated exceptional long-term cyclability (1600 h at 1 mA cm^{-2}) with an ultra-low overpotential (12.1 mV). The symmetrical cell tests at -10 °C, 25 °C, and 50 °C confirmed a wide temperature window, achieving 160, 350, and 500 h cycling at 2 mA cm^{-2}, respectively.

Electrode design with 3D hierarchical porous architecture has several advantages in reaching higher performance of SIBs. Rui *et al.* introduced amorphous carbon skeleton to design SIBs consisting of 3D porous NVP/C (NVP/C–F) and $NaTi_2(PO_4)_3$/C (NTP/C–F) foams for low-temperature operation.[58] The first-principles calculations revealed that the NTP/CF‖NVP/CF full cell demonstrates exceptional Na^+ diffusivity at -20 °C, with maximum values of 3.84×10^{-5} cm^2 s^{-1} for NVP and 2.94×10^{-9} cm^2 s^{-1} for NTP. This exhibited excellent low-temperature performance, achieving reversible capacities close to theoretical values and maintaining stability over 1000 cycles at -20 °C, even at high charge/discharge rates (20C).

4. Separator modification

To enhance battery performances in expansive temperature conditions, separator engineering has been applied to improve ionic transport and maintain mechanical integrity. Advanced separators are designed to suppress detrimental effects such as polysulfide diffusion and lithium dendrite formation, which are exacerbated at low temperatures due to sluggish reaction kinetics and increased electrolyte viscosity. Key strategies involve surface functionalization, incorporation of conductive and catalytic materials, and structural optimization to improve ionic conductivity and charge transfer efficiency.

Parekh *et al.* developed a graphene-polydopamine (PDA)-coated separator for the Li–S battery to enable a stable operation across a wide temperature range from -25 °C to 50 °C.[59] The tailored separator suppresses polysulfide diffusion by adsorbing soluble species (Fig. 4p), reducing shuttle-induced capacity fade. Using galvanostatic cycling tests, Li–S cells with the modified separator retained 170 mA h g^{-1} at -25 °C and exhibited stable operation, delivering 350, 580, 360, and 550 mA h g^{-1} at 0, 25, 40, and 50 °C, respectively. The batteries retained 95% capacity at C/2 after being cycled at 3C and 4C, demonstrating superior rate capability. Compared to a pristine polypropylene (PP) separator, the graphene-PDA treatment enhanced Li^+ transport, improving wettability and charge transfer efficiency (Fig. 4q–s). The tailored separator also suppressed lithium dendrite formation, promoting stable cycling over 400 cycles at high temperatures (40–50 °C). Pouch cell tests validated that Li–S cells maintained stable cycling at -10 °C, confirming the practicality of the separator modification for large-scale applications.

A similar study by Chen *et al.* reported a novel multifunctional separator with urchin-like Co-doped FeOOH microspheres and multiwalled carbon nanotubes (MWCNTs) as an

interlayer for Li–S battery to suppress the polysulfide shuttle and expand the operating temperature range from −25 °C to 100 °C.[60] To date, research on separator modifications specifically targeting wide-temperature battery applications remains scarce, posing a significant demand for effective separator modification strategies.

5. Summary and perspectives

As we move forward into an electrified future, battery researchers are facing more critical challenges in designing efficient and stable power devices that can operate in extreme conditions, such as cold climate outdoors, arctic, aerospace, and military applications. However, extreme temperature severely impacts the performance of both LIBs and SIBs by causing electrolyte freezing, sluggish ion diffusion, unstable SEI formation, and Li/Na plating on the electrode. These would ultimately lead to severe problems, including increased charge-transfer resistance, voltage hysteresis, capacity and voltage degradation, and safety concerns. In such a context, this review presents a comprehensive overview of recent advancements in designing LIBs and SIBs to resolve the issues under low temperature.

(a) Electrolyte innovations are the key to enabling extreme environmental applications. Recent research has mainly focused on designing new solvation structures by introducing temperature-responsive solvents, opting for HCEs, LHCEs, and WSEs instead of conventional electrolytes. Significant improvements have also been made in controlling the temperature-adaptive interphase design and introducing quasi-solid-state polymer electrolytes. Lastly, HEEs, formulated by combining multiple salts and solvents, offer a promising strategy for tailoring critical physicochemical properties—such as optimizing ionic conductivity and viscosity, improving electrochemical stability, and increasing thermal resilience—thereby necessitating further exploration to advance battery performance across diverse operating conditions.

(b) Electrode materials and electrode–electrolyte interphases are vital components for determining the performance of LIBs and SIBs under extreme environments. Therefore, electrode material modifications have been carried out by introducing multicomponent materials, redesigning device microstructure, and optimizing interfaces and morphology. Moreover, state-of-the-art characterization techniques, including cryo-TEM, *in situ* XRD, X-ray absorption spectroscopy, and galvanostatic intermittent titration technique, are required to elucidate interspatial characteristics and phenomena.

(c) Recent studies have focused on system-level engineering, such as separator modifications, to enhance ionic transport, wettability, and mechanical integrity in batteries. Furthermore, mechanically robust separators with tailored porosity and thermal stability help maintain structural integrity and suppress dendrite growth during low-temperature cycling, contributing to both enhanced safety and electrochemical stability.

However, designing a battery for all climate conditions needs a deep knowledge of the target battery chemistry along with the electrolytes and electrodes to optimize the dynamics of ion solvation and interface across wide temperatures. Future research for wide temperature applications of LIBs and SIBs should focus on overcoming material limitations, optimizing electrochemical systems, and particularly emphasizing commercial scalability. This review outlines the prospects for advancing extreme temperatures batteries as follows:

(a) Electrolyte chemistry and interaction mechanisms: electrolyte design must prioritize molecular-level modeling of ion–ion, ion–solvent, and solvent–solvent interactions under extreme temperatures to engineer electrolytes with adaptive solvation structures. Highly conductive electrolytes often suffer from parasitic side reactions or unstable electrode interfaces; hence, research should focus on balancing conductivity improvement by addressing ion desolvation kinetics and mitigating degradation pathways.

(b) Hybrid and high-entropy electrolytes: hybrid-solvent strategies, where mixture of strongly and weakly solvating solvents enhances ion transport and electrode compatibility. Systematically optimizing solvent–salt–additive synergies, such as pairing ethers (weak solvation) with carbonates (strong solvation), could mitigate sluggish Na^+ diffusion and anode passivation issues of SIBs. Thermodynamically stable high-entropy electrolytes engineered with multi-component salt/solvent mixtures could leverage entropy-driven stabilization to maintain uniform solvation structures across extreme temperatures. To validate this design, it requires *in situ* spectroscopic techniques to track dynamic solvation changes and multi-component DFT models that incorporate salts/additives, moving beyond simple solvent-only simulations. These approaches aim to create electrolytes that balance ion mobility, interfacial stability, and temperature resilience, bridging the performance gap between Na-ion and mature Li-ion technologies.

(c) Thermal safety and real-world applications: to mitigate thermal risks in wide-temperature batteries, research must focus on identifying thermal runaway triggers, such as dendrite-induced internal short circuits, and developing intrinsically stable electrode/electrolyte systems. This involves integrating flame-retardant additives, self-healing separators, and thermally resilient electrodes to suppress exothermic reactions. Moreover, expanding testing beyond coin cells to application-relevant formats (*e.g.*, pouch, cylindrical cells) is critical to evaluate thermal behavior under realistic mechanical and thermal stresses. These efforts will ensure scalable, safe battery designs that withstand extreme conditions while maintaining performance.

(d) Computational-experimental synergy: DFT calculations of the highest occupied molecular orbital and lowest unoccupied molecular orbital levels are widely used for electrolyte screening. However, these calculations should be performed on realistic systems that consider the collective effects of all electrolyte components, including salts and additives. This would supplement the previous works that focused solely on the effects of the solvents, which had oversimplified the entire solvent system and overlooked the interaction between all the components, such as salts or additives.

(e) Collaborative development and validation: a collaborative approach involving academics, engineers, and industry partners

is crucial for the successful development and application of new low-temperature batteries, particularly in emerging fields like drone technology. To fully realize the potential of low-temperature batteries for sustainable solar, wind, and tidal energy storage, practical proof-of-concept demonstrations showcasing their effectiveness in real-world energy storage scenarios are essential.

(f) Application-specific engineering: battery designs must be tailored by their application to meet diverse operational demands. Developing batteries operable under low-temperature is application-specific, as electric cars, drones, airplanes, and space satellites each require batteries tailored to their unique operating temperature needs.

Achieving reliable battery performance across extreme temperature ranges demands a paradigm shift toward integrative, application-driven design rooted in both fundamental understanding and practical validation. By aligning molecular-scale insights with real-world constraints, the next generation of energy storage systems can be engineered not merely to survive, but to thrive under the most demanding environmental conditions.

Author contributions

Sung-Kwang Jung: investigation, writing – original draft, review and editing. Jyotirekha Dutta: investigation, writing – original draft, review and editing. Surendra K. Martha: supervision. Martin Byung-Guk Jun: supervision. Vilas G. Pol: conceptualization, supervision, writing – review and editing.

Data availability

No primary research results, software, or code have been included, and no new data were generated or analysed as part of this review.

Conflicts of interest

There are no conflicts to declare.

Acknowledgements

We gratefully acknowledge support from the Purdue-Korea Center of Operation and Research for Industry Advancement (CORIA), a collaborative hub advancing innovation and global partnerships in semiconductors, batteries, and future mobility through cutting-edge research and industry engagement. VGP sincerely thanks Program Manager Dr Corey Love for his support through the Naval Enterprise Partnership Teaming with Universities for National Excellence (NEPTUNE) program, Office of Naval Research (Grant #N000142412510) for the project 'Understanding the Role of Electrode–Electrolyte Interphases at Ultra-low Temperature Li-ion Batteries for Prototype Development'.

Notes and references

1 Z. Li, Y.-X. Yao, S. Sun, C.-B. Jin, N. Yao, C. Yan and Q. Zhang, *Angew. Chem.*, 2023, **135**, e202303888.
2 R. Hou, S. Guo and H. Zhou, *Adv. Energy Mater.*, 2023, **13**, 2300053.
3 Y. Zhang, Y. Lu, J. Jin, M. Wu, H. Yuan, S. Zhang, K. Davey, Z. Guo and Z. Wen, *Adv. Mater.*, 2024, **36**, 2308484.
4 Z. Huang, Z. Xiao, R. Jin, Z. Li, C. Shu, R. Shi, X. Wang, Z. Tang, W. Tang and Y. Wu, *Energy Environ. Sci.*, 2024, **17**, 5365–5386.
5 F. Zhang, B. He, Y. Xin, T. Zhu, Y. Zhang, S. Wang, W. Li, Y. Yang and H. Tian, *Chem. Rev.*, 2024, **124**, 4778–4821.
6 C. Che, F. Wu, Y. Li, Y. Li, S. Li, C. Wu and Y. Bai, *Adv. Mater.*, 2024, **36**, 2402291.
7 J. Hou, M. Yang, D. Wang and J. Zhang, *Adv. Energy Mater.*, 2020, **10**, 1904152.
8 M.-T. F. Rodrigues, G. Babu, H. Gullapalli, K. Kalaga, F. N. Sayed, K. Kato, J. Joyner and P. M. Ajayan, *Nat. Energy*, 2017, **2**, 17108.
9 Y. Zhang, Y. Lu, J. Jin, M. Wu, H. Yuan, S. Zhang, K. Davey, Z. Guo and Z. Wen, *Adv. Mater.*, 2024, **36**, 2308484.
10 X. Zhu and L. Wang, *EcoMat*, 2020, **2**, e12043.
11 H. V. Ramasamy, S. Kim, E. J. Adams, H. Rao and V. G. Pol, *Chem. Commun.*, 2022, **58**, 5124–5127.
12 C. M. Jamison, S. Kim, H. V. Ramasamy, T. E. Adams and V. G. Pol, *Energy Technol.*, 2022, **10**, 2200799.
13 S. Kim, Y. Zhang, H. Wang, T. E. Adams and V. G. Pol, *Small*, 2024, **20**, 2306438.
14 S. Das, M. Bhuyan, K. N. Gupta, O. Okpowe, A. Choi, J. Sweeny, D. Olawale and V. G. Pol, *Small*, 2024, **20**, 2311850.
15 Z. Cui, D. Wang, J. Guo, Q. Nian, D. Ruan, J. Fan, J. Ma, L. Li, Q. Dong, X. Luo, Z. Wang, X. Ou, R. Cao, S. Jiao and X. Ren, *J. Am. Chem. Soc.*, 2024, **146**, 27644–27654.
16 X. Zheng, Z. Cao, W. Luo, S. Weng, X. Zhang, D. Wang, Z. Zhu, H. Du, X. Wang, L. Qie, H. Zheng and Y. Huang, *Adv. Mater.*, 2023, **35**, 2210115.
17 L. Luo, K. Chen, H. Chen, H. Li, R. Cao, X. Feng, W. Chen, Y. Fang and Y. Cao, *Adv. Mater.*, 2024, **36**, 2308881.
18 M. Wang, L. Yin, M. Zheng, X. Liu, C. Yang, W. Hu, J. Xie, R. Sun, J. Han, Y. You and J. Lu, *Nat. Commun.*, 2024, **15**, 8866.
19 C. Yang, X. Liu, Y. Lin, L. Yin, J. Lu and Y. You, *Adv. Mater.*, 2023, **35**, 2301817.
20 S. Kim, B. Seo, H. V. Ramasamy, Z. Shang, H. Wang, B. M. Savoie and V. G. Pol, *ACS Appl. Mater. Interfaces*, 2022, **14**, 41934–41944.
21 S. Kim and V. G. Pol, *ChemSusChem*, 2023, **16**, e202202143.
22 J. S. Packard, E. A. Adams and V. G. Pol, *Batteries*, 2024, **10**, 448.
23 E. Adams, M. Parekh, D. Gribble, T. Adams and V. G. Pol, *Sustainable Energy Fuels*, 2023, **7**, 3134–3141.
24 Z. Li, H. Rao, R. Atwi, B. M. Sivakumar, B. Gwalani, S. Gray, K. S. Han, T. A. Everett, T. A. Ajantiwalay, V. Murugesan, N. N. Rajput and V. G. Pol, *Nat. Commun.*, 2023, **14**, 868.
25 G. Song, Z. Yi, F. Su, L. Xie, Z. Wang, X.-X. Wei, G. Xu and C.-M. Chen, *ACS Energy Lett.*, 2023, **8**, 1336–1343.
26 J. Holoubek, K. Kim, Y. Yin, Z. Wu, H. Liu, M. Li, A. Chen, H. Gao, G. Cai, T. A. Pascal, P. Liu and Z. Chen, *Energy Environ. Sci.*, 2022, **15**, 1647–1658.
27 N. Chen, M. Feng, C. Li, Y. Shang, Y. Ma, J. Zhang, Y. Li, G. Chen, F. Wu and R. Chen, *Adv. Funct. Mater.*, 2024, **34**, 2400337.
28 S. Lin, H. Hua, P. Lai and J. Zhao, *Adv. Energy Mater.*, 2021, **11**, 2101775.
29 Y. Li, Y. Yang, Y. Lu, Q. Zhou, X. Qi, Q. Meng, X. Rong, L. Chen and Y.-S. Hu, *ACS Energy Lett.*, 2020, **5**, 1156–1158.
30 R. Jiang, L. Hong, Y. Liu, Y. Wang, S. Patel, X. Feng and H. Xiang, *Energy Storage Mater.*, 2021, **42**, 370–379.
31 Y.-H. Feng, M. Liu, J. Wu, C. Yang, Q. Liu, Y. Tang, X. Zhu, G.-X. Wei, H. Dong, X.-Y. Fan, S.-F. Chen, W. Hao, L. Yu, X. Ji, Y. You, P.-F. Wang and J. Lu, *Angew. Chem., Int. Ed.*, 2024, **63**, e202403585.
32 G. A. Giffin, *Nat. Commun.*, 2022, **13**, 5250.
33 H. Fang, Y. Huang, W. Hu, Z. Song, X. Wei, J. Geng, Z. Jiang, H. Qu, J. Chen and F. Li, *Angew. Chem.*, 2024, **136**, e202400539.
34 J. Zhou, Y. Wang, J. Wang, Y. Liu, Y. Li, L. Cheng, Y. Ding, S. Dong, Q. Zhu, M. Tang, Y. Wang, Y. Bi, R. Sun, Z. Wang and H. Wang, *Energy Storage Mater.*, 2022, **50**, 47–54.
35 D. Yu, Z. Wang, J. Yang, Y. Wang, Y. Li, Q. Zhu, X. Tu, D. Chen, J. Liang, U. Khalilov and H. Wang, *Small*, 2024, **20**, 2311810.
36 A. C. Thenuwara, P. P. Shetty, N. Kondekar, C. Wang, W. Li and M. T. McDowell, *J. Mater. Chem. A*, 2021, **9**, 10992–11000.

37 Y. Li, J. Wang, Y. Wang, S. Wang, L. Wu, B. Zhou, D. Yang, L. Jiang, L. Kan, Q. Zhu, M. Kurbanov and H. Wang, *Adv. Mater.*, 2025, **37**, 2419764.
38 X. Liu, X. Zheng, X. Qin, Y. Deng, Y. Dai, T. Zhao, Z. Wang, H. Yang and W. Luo, *Nano Energy*, 2022, **103**, 107746.
39 H.-J. Liang, H.-H. Liu, X.-X. Zhao, Z.-Y. Gu, J.-L. Yang, X.-Y. Zhang, Z.-M. Liu, Y.-Z. Tang, J.-P. Zhang and X.-L. Wu, *J. Am. Chem. Soc.*, 2024, **146**, 7295–7304.
40 J. Li, Q. Yuan, Y. Chen, Z. Zhang, Y. Yin, T. Wang, C. Wang, W. Mai and J. Li, *Adv. Funct. Mater.*, 2025, **35**, 2415680.
41 S. Das, V. G. Pol and V. Adyam, *J. Power Sources*, 2024, **617**, 235160.
42 Y. He, X. Shan, Y. Li, Z. Li, L. Li, S. Zhao, S. Gao, J. Qu, H. Yang and P.-F. Cao, *Energy Storage Mater.*, 2024, **68**, 103281.
43 Z. Li, R. Yu, S. Weng, Q. Zhang, X. Wang and X. Guo, *Nat. Commun.*, 2023, **14**, 482.
44 J. Yu, X. Lin, J. Liu, J. T. T. Yu, M. J. Robson, G. Zhou, H. M. Law, H. Wang, B. Z. Tang and F. Ciucci, *Adv. Energy Mater.*, 2022, **12**, 2102932.
45 G. Wang, G. Wang, L. Fei, L. Zhao and H. Zhang, *Nano-Micro Lett.*, 2024, **16**, 150.
46 J. H. Kim, S. Kim, Y. C. Kang and V. G. Pol, *Nano Energy*, 2024, **128**, 109823.
47 H. V. S. R. M. Koppisetti, H. Rao, H. V. Ramasamy, H. R. Inta, S. Das, S. Kim, Y. Zhang, H. Wang, V. Mahalingam and V. G. Pol, *ACS Appl. Mater. Interfaces*, 2023, **15**, 32291–32300.
48 M. Chen, W. Hua, J. Xiao, D. Cortie, W. Chen, E. Wang, Z. Hu, Q. Gu, X. Wang, S. Indris, S.-L. Chou and S.-X. Dou, *Nat. Commun.*, 2019, **10**, 1480.
49 S. Zhao, G. Li, Z. Li, K. Zhang, X. Chen, X. Dong, Y. Wang, Y. Cao and Y. Xia, *Adv. Funct. Mater.*, 2025, **35**, 2411007.
50 Z. Li, Y. Zhang, J. Zhang, Y. Cao, J. Chen, H. Liu and Y. Wang, *Angew. Chem., Int. Ed.*, 2022, **61**, e202116930.
51 C. Wang, D. Du, M. Song, Y. Wang and F. Li, *Adv. Energy Mater.*, 2019, **9**, 1900022.
52 Y. Tian, J. Lu, H. Tang, X. Wang, L. Zhang, P. Hu, L. Zhou, Y. Wang, Y. Guo, R. Khatoon, Q. Zhang, Q. He, Y. He, M. Qiu, Y. Hou and Z. Ye, *Chem. Eng. J.*, 2021, **422**, 130054.
53 A. Varzi, L. Mattarozzi, S. Cattarin, P. Guerriero and S. Passerini, *Adv. Energy Mater.*, 2018, **8**, 1701706.
54 P. Yadav, A. K. Das, A. Torris, K. Wasnik, H. V. S. R. M. Koppisetti, V. G. Pol, V. Shelke and M. Shelke, *Mater. Today Chem.*, 2024, **37**, 101978.
55 T. Jiang, S. Ma, J. Deng, T. Yuan, C. Lin and M. Liu, *Adv. Sci.*, 2022, **9**, 2105119.
56 T. Lyu, F. Luo, L. Liang, D. Wang, L. Tao and Z. Zheng, *Adv. Energy Mater.*, 2024, **14**, 2304520.
57 J. Wang, M. Yang, J. Wang, D. Liu, G. Zou, B. Liu, J. S. Tse, L. Li, L. Ren and Q. Peng, *Energy Storage Mater.*, 2022, **47**, 611–619.
58 X. Rui, X. Zhang, S. Xu, H. Tan, Y. Jiang, L. Y. Gan, Y. Feng, C. C. Li and Y. Yu, *Adv. Funct. Mater.*, 2021, **31**, 2009458.
59 M. H. Parekh, H. Rao, D. Jokhakar, V. P. Parikh, M. Palanisamy and V. G. Pol, *Sustainable Energy Fuels*, 2022, **6**, 5591–5599.
60 X.-S. Chen, Y. Gao, G.-R. Zhu, H.-J. Chen, S.-C. Chen, X.-L. Wang, G. Wu and Y.-Z. Wang, *J. Energy Chem.*, 2020, **50**, 248–259.